Energy implications of control strategies in ventilated façades

M. Haase
SINTEF Building and Infrastructure, 7465 Trondheim, Norway

F. Marques da Silva
Laboratório Nacional de Engenharia (LNEC), Civil Structures Department, Lisboa, Portugal

A. Amato
Davis Langdon Management Consulting, MidCity Place, London WC1V 6QS

ABSTRACT

Thermal building simulations (TRNSYS) were linked to nodal airflow network simulations (COMIS) for a detailed ventilated double-skin facade calculation of performance. The validated simulation model can be used to optimize the ventilated facade design in respect to reducing the solar heat gains during the summer period by controlling the exhaust airflow. This may result in significant energy savings and a reduction in systems cooling size. This work evaluates two different control strategies of ventilated façade designs in respect to cooling load reductions. Different control strategies can help to reduce cooling load of an office up to almost 40%.

1. INTRODUCTION

The development of advanced integrated facades (AIF) technology involves several advantages by improving the thermal, visual and acoustic comfort (Oesterle et al., 2001). In moderate climates the air layer helps to insulate the building and thus reduce the energy consumption for heating. This is more significant in cool climates with strong winter periods (Balocco, 2002; Park, 2003). Then, it creates a space for advanced sunshading devices. Positioned into the cavity of the AIF it seems to influence heat gain (von Grabe, 2002). Furthermore the buoyancy flow in the cavity itself may reduce solar heat gain and additionally it can support the HVAC-system (heating, ventilation and air-conditioning) and it can help to minimize the size of the system and consequently the energy consumption of the building (Saelens et al., 2003; Stec, 2001; Stec and Paassen, 2005). However, little work has been done on control strategies in AIF for hot and humid climates (Haase and Amato, 2005).

1.1 Advanced integrated façade concept

Many types of AIFs have been developed since the first double layer was used in the building envelope (Annex44, 2006b; Parkin, 2004). It can be classified by the following criteria:

- Type of ventilation
- Air flow path
- Façade configuration

Figure 1 gives a classification of the façade configuration often used when describing the various features of AIFs. It is important to note that all main types of AIFs can be combined with all types of ventilation and all types of airflow paths. This produces a great variety of AIFs. More recently, AIF have been developed that act as climate responsive elements with hybrid ventilation (natural and mechanical) concepts with a possibility to change the airflow concept due to different weather conditions in different seasons (Heiselberg et al., 2001).

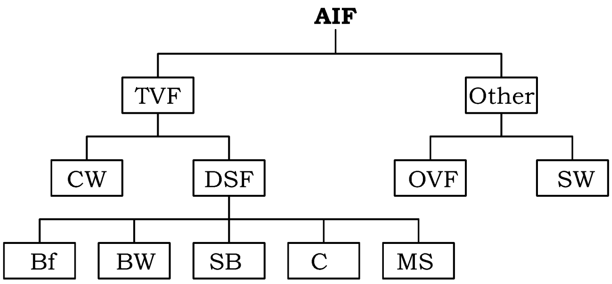

Figure 1. Classification of AIF (Annex44, 2006b)

1.2 AIF performance

The heat transfer through the buildings envelope depends on solar radiation, conduction and convection of the airflow through the double-skin gap. The convection in the cavity depends on the airflow. Several possible calculation models have been developed to simulate the thermal behavior of double-skin facades (Manz, 2003; Saelens et al., 2003; Stec and Paassen, 2005). One problem is to use dynamic building simulation with hourly weather data on the one hand but also to take the effects of airflow in the cavity into account. The airflow affects the heat transfer but is also influenced by external wind conditions (and the pressure it creates on the building envelope).

A new model has been set up that is based on the Star network method implemented by Seem (1987) and validated by Holst (1993) to determine zone temperatures (Holst, 1993; Seem, 1987). These are directly linked to energy calculation for cooling the room (including internal heat gains from people, light, and office equipment).

The convective heat transfer from the internal shading device has been taken into consideration by

$$\dot{q}_{conv,sh} = \dot{q}_{int,sh}\, c_{conv,sh} \quad (1)$$

with

$$\dot{q}_{int,sh} = \left[\begin{array}{l} f_{int,sh}(1 - refl_{sh,o}) + (1 - f_{int,sh}) \times \\ \times \left(\dfrac{refl_{win,i} f_{int,sh} (1 - refl_{sh,i})}{1 - refl_{win,i} f_{int,sh} refl_{sh,i}} \right) \end{array} \right] I_{ref,z} + trans_{win} \left(\dfrac{f_{int,sh}(1 - refl_{sh,i})}{1 - f_{int,sh} refl_{sh,i} refl_{win,i}} \right) I \quad (2)$$

where

$f_{int,sh}$ = non transparent fraction of internal shading related to the total glass area
$refl_{sh,i}$ = solar reflection of internal shading facing the glass
$refl_{sh,o}$ = solar reflection of internal shading facing the room
$refl_{win,i}$ = solar reflection of glass surface facing the internal shading device
$trans_{win}$ = solar transmittance of all window panes
$c_{conv,sh}$ = convective heat transfer coefficient
I = incident solar radiation
$I_{ref,z}$ = reflected solar radiation
$\dot{q}_{conv,sh}$ = convective heat transfer to zone
$\dot{q}_{int,sh}$ = heat transfer from internal shading

Two zones describe the AIF and one zone is representing the office room. All three zones have been coupled with a nodal network determining coupled airflow through all three zones (Haas et al., 2002).

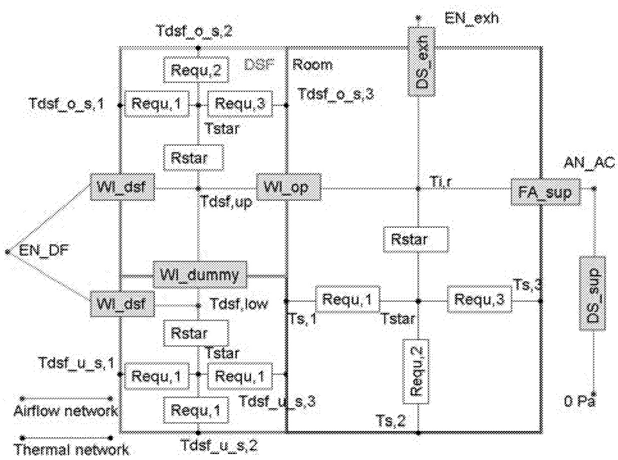

Figure 2. Coupled thermal and airflow of the EAC model

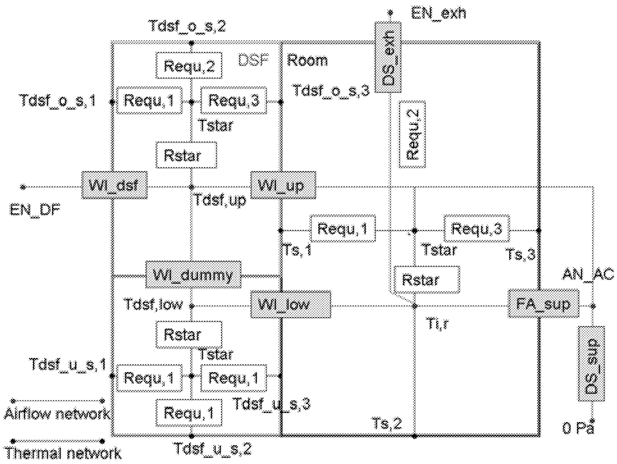

Figure 3. Coupled thermal and airflow of the IAC model

Both heat transfer and airflow calculations were performed iteratively to determine temperatures at the lower and upper part of the DSF (Tdsf,low and Tdsf,up) and in the room (Ti,r). The simulation accuracy of the DSF system has been validated with measured data (Haase et al., 2007). It showed good agreement between detailed measured and simulated surface temperatures.

2. OBJECTIVES

This study tried to find out the influence of different control strategies for DSF on the cooling load of an office room in a warm and humid climate. Two DSF systems have been simulated (IAC and EAC) and two control strategies have been compared: control of the shading system and of the airflow in the cavity. The objective was to find the control strategy which minimized cooling load performance of the office room for the whole year and the hottest month.

3. METHODOLOGY

Three models were set up with different control strategies to compare their performance. The first model is a curtain wall system with reflective glazing which is common in HK. It acts as a base case for comparison and the consequences of different types of glazing have been reported (Haase and Amato, 2006).

The second model an external air curtain (EAC) with 600mm depth gap with one-storey cavity. The EAC is open on bottom and top to the outside allowing a naturally ventilated cavity. Details are shown in Figure 2. A solar controlled shading device is positioned in the cavity (EAC1). The internal window is openable according to an enthalpy control strategy which is described below.

The third model is a mechanical ventilated internal air curtain with a cavity depth of 240mm. Both glass layers were selected as single clear glass (8mm) with a shading device positioned in the cavity.

Two climate responsive control strategies have been simulated as summarized in Table 1. The first is to control the airflow direction (from internal to external or vice versa) and flow rate. It compared the room enthalpy with cavity enthalpy. The enthalpies in the room, in the cavity, and outside were calculated. Depending on the type of DSF enthalpy differences were calculated and the window openings controlled. For the EAC a comparison between room enthalpy (hr) and cavity enthalpy (hc) was done. The window (WI_op) between cavity and room was opened if hr>hc. In the IAC a damper opened to the exterior (WI_dsf) when the cavity enthalpy (hc) was higher then external enthalpy (he) in order to exhaust the air (see Figure 3).

The second strategy is to control the shading system. The amount of solar radiation on the facade is used to shade the window accordingly. The shading closed when the incident solar radiation exceeded 200 W/m^2 and opened when it dropped below 150 W/ m^2 (150 – 100, 100 – 50, 50 – 0, respectively).

Table 1. Control strategies

Option	airflow control		shading control	Annual cooling load
	fan flow rate $[\frac{l}{s}]$	Enthalpy criteria opening	Down – up $[\frac{W}{m^2}]$	$[\frac{kWh}{m^2 y}]$
BC1		-	-	155,40
BC2		-	200-150	148,28
BC3		-	150-100	146,7
BC4		-	100-50	145,9
BC5		-	50-0	145,2
EAC1		-	-	146,0
EAC2		-	200-150	120,0
EAC3		-	150-100	115,7
EAC4		-	100-50	113,6
EAC5		-	50-0	114,7
EAC6		hr > hc	-	118,7
EAC7		hr > hc	200-150	101,0
EAC8		hr > hc	150-100	97,7
EAC9		hr > hc	100-50	95,7
EAC10		hr > hc	50-0	96,8
IAC1	-	-	-	181,7
IAC2	-	-	200-150	161,3
IAC3(*)	-	hc > he	200-150	154,0
IAC4	96	hc > he	200-150	117,6
IAC5	144	hc > he	200-150	109,7
IAC6	192	hc > he	200-150	101,6
IAC7	192	hc > he	50-0	98,4
IAC8	288	hc > he	200-150	94,7
IAC9	384	hc > he	200-150	89,7

Note: (*) External window opens but no exhaust fan is provided. This will lead to uncontrolled airflow.

4. RESULTS

Simulations of the room cooling loads were done for the whole year. The results shown in Table 1 give the annual cooling load per floor area for the different façade options with different control strategies. It illustrates the influence of control strategy in relationship to different façade systems.

It can be seen from Table 1 and Figure 4 that the base cases (BC1-BC5) result in a simulated cooling load between 148 and 145 kWh/m^2/y. This is an improvement of 6.6 % between BC5 and BC1 due to the introduction and optimization of a solar control that lowers the shading device when the solar radiation is more than 50W/m^2.

The different control strategies for EAC result in annual cooling loads between 96 and 146 kWh/m^2/y. There is a reduction from EAC1 to EAC2 of 26 kWh/m^2/y due to the introduction of a solar control. Further reductions in cooling load are possible by further reducing the amount of solar radiation on the façade (EAC3 to EAC4). A further reduction to 50W/m2 (EAC5) does not decrease the cooling load further. The EAC with additional airflow control (EAC6 to EAC10) are significantly reducing cooling load compared to EAC without this control (EAC1 to EAC5). There is an improvement between EAC1 and EAC6 of 27 kWh/m^2/y due to the introduction of a airflow control. Further reductions in cooling load are possible by introducing a solar control (EAC7 to EAC10).

The IAC without airflow and shading control increases annual cooling load to 182 kWh/m^2/y (IAC1). With internal shading control the annual cooling load decreases to 161 kWh/m^2/y which is still higher than BC1. This is due to the clear glazing in all the DSF cases and the reflective glazing for the BC. The introduction of an airflow control (with openings to the exterior) decreases annual cooling load to 154kWh/m^2 (IAC2). If the exhaust is ensured (here by the addition of a fan) the cooling load can be reduced to 90 kWh/m^2/y (IAC8) which is 44 kWh/m^2/y compared to IAC1. But an increase of airflow is inherent with an increase of fan power. With a specific fan power of 2 W/l/s and daily 4 hours usage and an additional 192l/s (384l/s respectively) this accounts for additional fan electricity consumption of 7.5kWh/m^2/y (15kWh/m^2/y respectively).

Figure 4 gives the percentage of cooling load reduction for the whole year and for the hottest month. Here, BC1 was taken as a reference. It can be seen that the different options reduce annual cooling load between 1% and 42%.

EAC reduce annual cooling load between 6% (EAC1) and 38% (EAC9) and for the hottest month between 26% (EAC1) and 36% (EAC10). Solar control strategy reduces annual cooling load for about 4% and for the hottest month

IAC change annual cooling load between -17% (IAC1) and 42% (IAC8) and for the hottest month between -9% (IAC2) and 40% (IAC6).

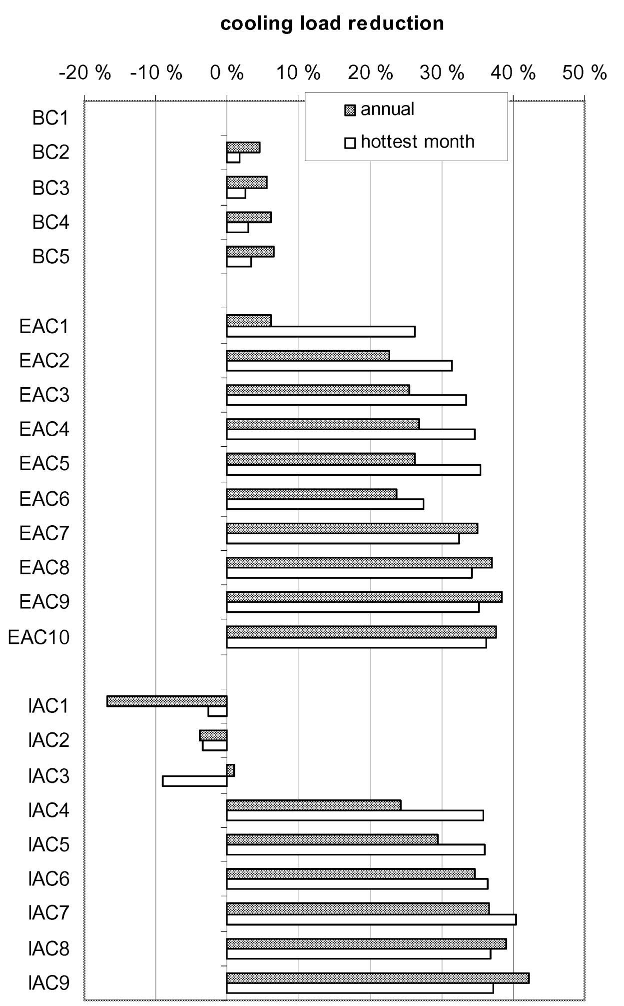

Figure 4. Cooling load reductions for whole year and hottest month (August)

5. CONCLUSIONS

The influence of different control strategies for DSF on the cooling load of an office room in a warm and humid climate have been estimated. Two DSF systems have been simulated (IAC and EAC) and two control strategies have been compared: control of the shading system and of the airflow in the cavity. The control strategy which minimized cooling load performance of the office room for the whole year and the hottest month could be identified.

For the base case curtain wall system a solar control can be applied. The results for BC1 to BC5 show the effectiveness of the applied control strategy.

The EAC uses natural ventilation in the cavity to reject heat gain. An EAC system has the potential of reducing cooling load even without applying control strategies (comparing EAC1 with BC1 provides 6% reduction in annual cooling load). The performance of the EAC can further be reduced by applying an enthalpy control of the the cavity airflow. This mainly reduces cooling loads during winter months (with lower external enthalpy). The best results for annual cooling load of an EAC are observed for EAC9 with strict solar control but EAC10 gives the best result for the hottest month.

The IAC does not reduce the cooling load of the office room unless an enthalpy based control is used that extracts air in order reduce the cooling load of an office room. This system is giving the best results for the solar control strategy of lowering the shading device at 200W/m^2 and lifting it at 150W/m^2. Further reductions are possible if the solar control strategy is more stringent and uses 100W/m^2 for lowering the shading device. Further reducing the amount of solar radiation to control the shading device does not reduce cooling load. Solar control strategy has a smaller influence on cooling load reduction. A high fan flow rate means a high cooling load reduction but is penalized by an increase in fan energy consumption.

While a reduction of radiation is met by using controlled solar shading devices, there are constraints from maximizing the use of daylight. Further research is planned to optimize the

amount of daylight and thus reduce internal heat gain.
For IAC the importance of an airflow control based on enthalpy of the air was demonstrated.

6. ACKNOWLEDGEMENTS

The majority of this work was done at the Department of Architecture, the University of Hong Kong and the financial help is greatfully acknowledged. Further, this work is part of the International Energy Agency, Energy conservation in buildings and community systems (Annex44, 2006a). Fruitful discussions of parts of the work among the participants are highly appreciated.

7. REFERENCES

Annex44, 2006a. Introduction to the Annex44 work - Scope and objectives, in: Heiselberg, P. (Ed.), Integrating responsive building elements in buildings. International Energy Agency I. E. A., Energy Conservation in Buildings and Community Systems Programme.

Annex44, 2006b. State of the Art report, in: Heiselberg, P. (Ed.), Integrating responsive building elements in buildings. International Energy Agency I. E. A., Energy Conservation in Buildings and Community Systems Programme.

Balocco, C., 2002. A simple model to study ventilated facades energy performance. Energy and Buildings 34, 469-475.

Heiselberg, P., Svidt, K., Nielsen, P.V., 2001. Characteristics of airflow from open windows. Building and Environment 36, 859-869.

Holst, S., 1993. Heating load of building model in TRNSYS with different heating systems, TRNSYS User Days. Transsolar, Stuttgart.

Haas, A., Weber, A., Dorer, V., Keilholz, W., Pelletret, R., 2002. COMIS v3.1 simulation environment for multizone air flow and pollutant transport modelling. Energy and Buildings 34, 873-882.

Haase, M., Amato, A., 2005. Double-skin facades in Hong Kong, 5th International Postgraduate Research Conference. University of Salford, Salford, U.K.

Haase, M., Amato, A., 2006. Design considerations of double-skin facades in hot and humid climates, International Conference on Enhanced Building Operation. ICEBO, Shenzhen, PRC.

Haase, M., Marquez da Silva, F., Amato, A., 2007. Model validation of double-skin façade simulation, Sustainable Building conference 2007 (SB07), Hong Kong SAR.

Manz, H., 2003. Numerical simulation of heat transfer by natural convection in cavities of facade elements. Energy and Buildings 35, 305-311.

Oesterle, E., Lieb, R.-D., Lutz, G., Heusler, B., 2001. *Double-skin facades : integrated planning : building physics, construction, aerophysics, air-conditioning, economic viability*. Prestel, Munich.

Park, C.-S., 2003. Occupant-Responsive optimal control of smart facade systems, Department of Architecture. Georgia Institute of Technology, p. 350 p.

Parkin, S., 2004. A description of a ventilated double-skin façade classification, International Conference on Building Envelope Systems & Technology. ICBEST2004 Pty Ltd, Sydney, Australia.

Saelens, D., Carmeliet, J., Hens, H., 2003. Energy performance assessment of multiple skin facades. International Journal of HVAC&Research 9, 167-186.

Seem, J.E., 1987. Modeling of heat transfer in buildings, Solar Energy Laboratory, University of Wisconsin-Madison. University of Wisconsin-Madison, Wisconsin.

Stec, W., van Paassen, A. H. C., 2001. Controlled double facades and HVAC, 7th Clima 2000 World Congress, Napoli (I).

Stec, W.J., Paassen, A.H.C.v., 2005. Symbiosis of the double skin facade with the HVAC system. Energy and Buildings 37, 461-469.

von Grabe, J., 2002. A prediction tool for the temperature field of double facades. Energy and Buildings 34, 891-899.